Analysis and simulation of a 4H-SiC semi-superjunction Schottky barrier diode for softer reverse-recovery*

Cao Lin(曹 琳)†, Pu Hong-Bin(蒲红斌), Chen Zhi-Ming(陈治明), and Zang Yuan(臧 源)

Department of Electronic Engineering, Xi'an University of Technology, Xi'an 710048, *China*

(Received 24 March 2011; revised manuscript received 5 May 2011)

In this paper, a 4H-SiC semi-superjunction (SJ) Schottky barrier diode is analysed and simulated. The semi-SJ structure has an optimized design and a specific on-resistance lower than that of conventional SJ structures, which can be achieved without increasing the process difficulty. The simulation results show that the specific on-resistance and the softness factor depend on the aspect and thickness ratios, and that by using the semi-SJ structure, specific on-resistance can be reduced without decreasing the softness factor. It is observed that a trade-off exists between the specific on-resistance and the softness of the diode.

Keywords: 4H-SiC, semi-superjunction, Schottky barrier diode, softness factor

PACS: 73.30.+y, 73.40.Sx **DOI:** 10.1088/1674-1056/21/1/017303

1. Introduction

The silicon carbide (SiC) Schottky barrier diode (SBD) was the first SiC power device, and was demonstrated as early as 1974.[1] Throughout the years, a great deal of work has been done on SiC SBDs, as well as merged P–i–N Schottky (MPS) diodes and junction barrier Schottky diodes. Schottky contacts on 3C, 6H and 4H SiC with a large variety of metals were also extensively investigated. An SiC SBD with a breakdown voltage higher than 10 kV has been reported,[2] along with an SiC MPS with a breakdown voltage of 4.3 kV,[3] and it is possible to replace the existing Si power fast recovery diode in most power electronic applications because of its greatly improved speed, substantially reduced system losses and improved system efficiency.

The superjunction (SJ) structure[4−7] is based on a charge compensation concept that overcomes the trade-off between the blocking voltage ($V_{\rm br}$) and the specific on-resistance ($R_{\rm on_sp}$). The major difficulty in realizing a higher voltage SiC SJ structure is the increase in the process difficulty. Nevertheless, an SiC dry etching process to produce long and narrow n and p stripes has already been developed, and mesas and trenches with relatively high aspect ratios (i.e. a height-to-width ratio that is larger than 4:1) are already practically feasible.[8]

The drift region of the SJ structure is composed of multiple alternate n and p stripes. The stripes are fairly narrow, and the net dopings in the stripes are approximately equal. The stripes deplete at relatively low voltages, and therefore reverse-recovery hardness is obtained. The abrupt drop-off of current imposes stress on the other circuit transistors, leading to large electromagnetic interference (EMI) noise and high-power dissipation.

In this paper, a 4H-SiC Schottky barrier diode combined with an SJ structure and an n-bottom assist layer (BAL) – called the semi-superjunction[9−11] Schottky barrier diode (semi-SJ-SBD) – is analysed and simulated, and realizes both lower on-resistance and softer reverse-recovery characteristics compared with those of conventional SJ structures, without an increase in process difficulty.

2. Device structure analysis

The structure of a semi-SJ-SBD is the combination of an SJ structure and a BAL, as shown in Fig. 1.

The $V_{\rm br}$ and $R_{\rm on_sp}$ of the semi-SJ SBD are, respectively, the sums of the blocking voltages and the

*Project supported by the National Natural Science Foundation of China (Grant No. 60876050) and the Research Fund for Excellent Doctor Degree Thesis of Xi'an University of Technology, China.

†Corresponding author. E-mail: cl_zhifang@hotmail.com

© 2012 Chinese Physical Society and IOP Publishing Ltd

specific on-resistances of the SJ and BAL structures due to their series connections.

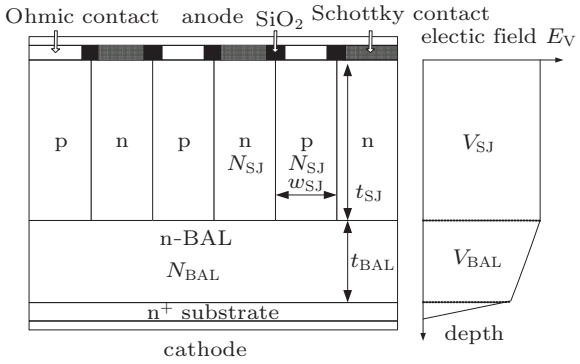


Fig. 1. A schematic cross section of a semi-superjunction Schottky diode.

For the SJ structure, the depleted region of the column is neglected, then the on-resistance and sustain voltage can be calculated from

$$R_{SJ} = \frac{2t_{SJ}}{q\mu N_{SJ}}, \tag{1}$$

$$V_{SJ} = E_V t_{SJ}, \tag{2}$$

where q is the charge of an electron, μ is electron mobility, N_{SJ} is the doping concentration of the p and n columns, and E_V is the vertical peak electric field. Considering the critical field E_C as a constant, then E_C will be given by[12]

$$E_C^2 = \left(\frac{V_{SJ}}{t_{SJ}}\right)^2 + \left(\frac{dqN_{SJ}b}{\varepsilon_s}\right)^2, \tag{3}$$

where d and b are the device parameters depending on the cell pattern design (hexagonal, interdigitated, square, lattice). For the highest breakdown voltage with the on-resistance minimized, both terms should be equal. For the interdigitated cell pattern, it turns out that

$$E_V = \frac{qN_{SJ}w_{SJ}}{2\varepsilon_s} = \frac{qN_{SJ}t_{SJ}}{2\varepsilon_s A_{SJ}} = \frac{E_C}{\sqrt{2}}, \tag{4}$$

where A_{SJ} is the aspect ratio of the p and n columns ($A_{SJ} = t_{SJ}/w_{SJ}$). From the above equation, the relation between V_{SJ} and R_{SJ} is given by

$$R_{SJ} = \frac{2\sqrt{2}V_{SJ}^2}{\varepsilon_s \mu E_C^3 A_{SJ}}. \tag{5}$$

For the BAL structure, R_{BAL} and sustain voltage V_{BAL} at the BAL are given by

$$R_{BAL} = \frac{t_{BAL}}{q\mu N_{BAL}}, \tag{6}$$

$$V_{BAL} = \left(E_V - \frac{qN_{BAL}t_{BAL}}{2\varepsilon_s}\right)t_{BAL}. \tag{7}$$

The BAL can be designed as a conventional Schottky drift layer, and so the optimized specific on-resistance is given by[13]

$$R_{BAL} = \frac{4V_{BAL}^2}{\varepsilon_s \mu E_C^3}. \tag{8}$$

Therefore, on-resistance $R_{semi-SJ}$ and breakdown voltage $V_{semi-SJ}$ are given by

$$\begin{aligned} R_{semi-SJ} &= R_{BAL} + R_{SJ} \\ &= \frac{1}{\varepsilon_s \mu E_C^3}\left[\frac{2\sqrt{2}V_{SJ}^2}{A_{SJ}} + 4(V_{semi-SJ} - V_{SJ})^2\right], \end{aligned} \tag{9}$$

$$V_{semi-SJ} = V_{SJ} + V_{BAL}. \tag{10}$$

The aspect ratio is determined by the process difficulty or the process step number. The optimized relations between R_{on_sp} and the thickness ratio $r_t = t_{SJ}/t_{semi-SJ}$ for some aspect ratios and a fixed V_{br} value are shown in Fig. 2. The semi-SJ-SBD realizes lower specific resistance than that of the SJ-SBD ($r_t = 1$) at the optimized thickness ratio with the same aspect ratio. The R_{on_sp} decreases with increasing aspect ratio or the optimizing thickness ratio. As shown in Fig. 3, both the SJ-SBD and the semi-SJ-SBD specific resistances decrease with the increasing aspect ratio, and the optimized thickness ratio increases with the decreasing aspect ratio. Therefore, the specific resistance of the semi-SJ-SBD is smaller than that of the SJ-SBD with the same aspect ratio.

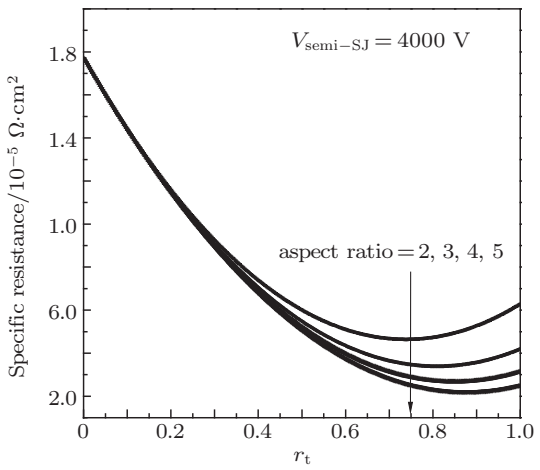


Fig. 2. The R_{on_sp} versus thickness ratio.

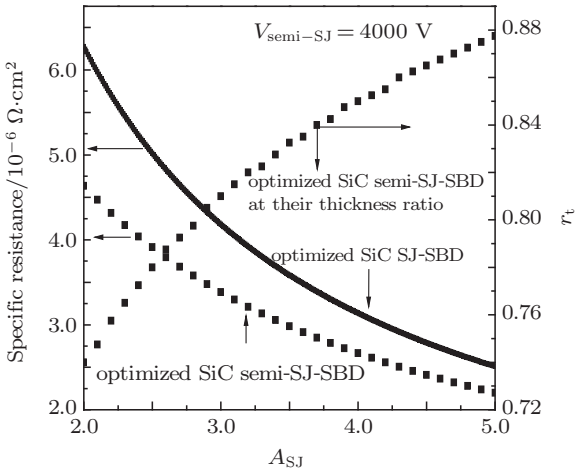


Fig. 3. The $R_{\text{on_sp}}$ and thickness ratio versus aspect ratio.

3. Reverse-recovery characteristics

The reverse-recovery characteristic are calculated with the mixed circuit-device simulator, MEDICI[14], under the inductive load.[15]

The reverse-recovery time, t_{rr}, is determined by the excess injected carrier extraction (t_{a}) to remove the dopant charge in the n and p columns of the drift region (t_{b}). It can be simply obtained as[16]

$$t_{\text{a}} = \sqrt{\frac{2Q}{\mathrm{d}i_{\text{F}}/\mathrm{d}t}}, \tag{11}$$

$$t_{\text{b}} = \frac{2NW_{\text{SJ}}}{I_{\text{RM}}}, \tag{12}$$

where Q is the charge of the excess injected carriers, N is the dopant charge in the n and p columns of the drift region, and $\mathrm{d}i_{\text{F}}/\mathrm{d}t = V_{\text{R}}/L$, $I_{\text{RM}} = t_{\text{a}} \times \mathrm{d}i_{\text{F}}/\mathrm{d}t$, and $V_{\text{RM}} = V_{\text{R}} \times L \times \mathrm{d}i_{\text{rr}}/\mathrm{d}t$.

Unlike conventional PiN diodes, the reverse bias is supported by the depletion layer at the p^+ edge. The SJ-SBD remains in the on-state simply due to the fact that the middle pn junction within the striped drift region is still forward biased, and the carrier extraction continues across the middle pn junction when the depletion layer forms progressively along the entire length of the middle junction from the anode to the cathode. Reverse recovery can be characterized by the expansion of the depletion region across the junction. The striped geometry of the SJ structure influences the flow of the injected carriers and the growth of the depletion layer during reverse recovery. The injected excess carriers are almost completely removed due to the depletion of the p and n columns at low reverse voltages, and a steep reduction in the capacitance is obtained. There is little or no stored charge left in the drift region of the diode, thus the reverse current flowing through the diode decreases very rapidly, and results in large $\mathrm{d}i_{\text{rr}}/\mathrm{d}t$, as shown in Fig. 4(a), which imposes stress (V_{RM}) on other circuit transistors and induces large EMI noise and high power dissipation. In the semi-SJ structure shown in Fig. 4(b), the additional BAL layer is gradually depleted after the depletion of the SJ structure at a high-reverse voltage. The junction capacitance decreases gradually, and so soft recovery characteristics are realized.

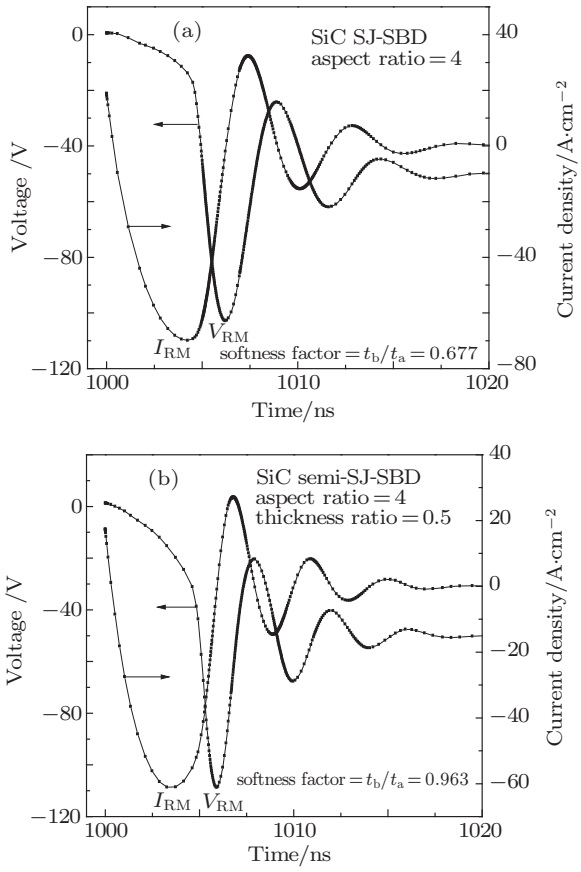


Fig. 4. Reverse-recovery waveforms of (a) SJ-SBD and (b) semi-SJ-SBD.

The softness factor decreases with the increases in the thickness ratio and the BAL doping concentration (N_{BAL}), because the BAL depletion is enhanced. Both $R_{\text{on_sp}}$ and the softness factor depend on the thickness ratio and the BAL doping concentration, so a trade-off must be made between them.

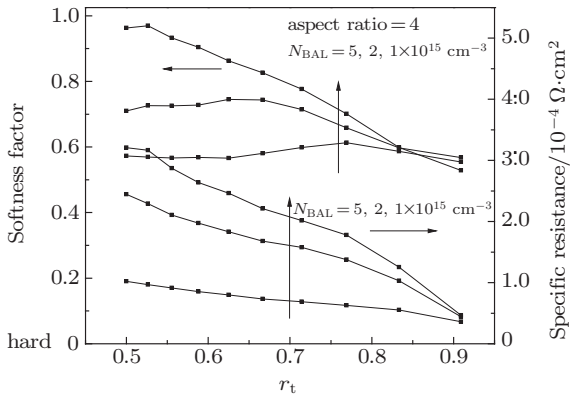


Fig. 5. The R_{on_sp} and softness factors versus thickness ratio at three BAL doping concentrations.

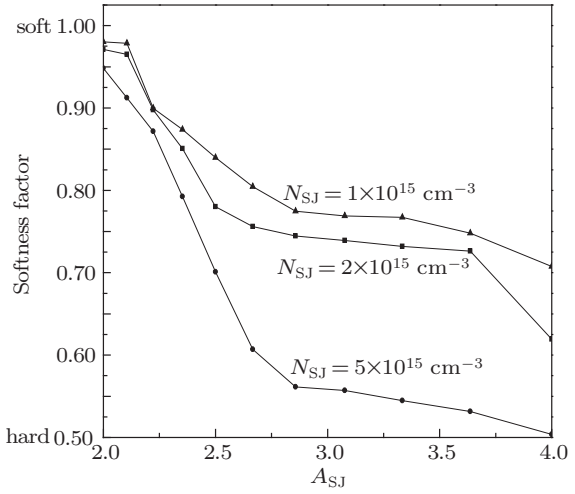


Fig. 6. Softness factors versus aspect ratio at three doping concentrations of the p and n columns.

The rise time, t_a, is the excess injected carrier extract time in the drift region, which is proportional to the length of the drift region. The fall time, t_b, is estimated as the time taken to remove the dopant charge in the n and p stripes of the drift region, and is proportional to the width of the drift region. Therefore, the softness becomes hard with the increasing aspect ratio at a constant drift region length. The SJ structure needs a high p/n column structure aspect ratio in order to obtain the low R_{on} to fulfill the charge compensation. This gives rise to conflicting requirements between the on-resistance and the softness factor.

4. Conclusion

A 4H-SiC semi-SJ-SBD is studied through analytical and numerical simulation methods. Due to the unique striped geometry of the SJ structure, a low specific on-resistance is achieved with highly doped narrow stripes, which are depleted at low voltages and thus hard reverse recovery is obtained. However, due to the bottom assistance layer in the 4H-SiC semi-SJ-SBD, the optimized semi-SJ-SBD achieves not only a lower on-resistance, but also soft recovery characteristics. The semi-SJ-SBD is therefore an effective way to reduce power dissipation and avoid EMI noise due to low on-resistance and soft recovery characteristics.

References

[1] Wu S Y and Campbell R B 1974 *Solid State Electron.* **17** 638

[2] ZHAO J H, Alexandrov P and Li X 2003 *Electron Device Lett.* **24** 402

[3] Wu J, Furisin L, Li Y, Alexandrov P and Zhao J H 2004 *Mat. Sci. Forum* **457** 1109

[4] Strollo A G M and Napoli E 2001 *Microelectronics J.* **32** 491

[5] Park Y, Andre C and Salama T 2006 *IEEE Trans. Electron Devices* **53** 8

[6] Yu L C and Sheng K 2006 *Solid State Electron.* **50** 1062

[7] Zhu L, Losee P and Chow T P 2004 *Int. J. High Speed Electron. Sys.* **14** 865

[8] Yu L C and Sheng K 2008 *IEEE Trans. Electron Devices* **55** 1961

[9] Antoniou M, Udrea F, Bauer F and Nistor I 2010 *IEEE Trans. Electron Devices* 31 591

[10] Saito W, Omura I, Aida S, Koduki S, Izumisawa M, Yoshioka H and Ogura T 2005 *IEEE Trans. Electron Devices* **52** 2317

[11] Yang Y T, Geng Z H, Duan B X, Jia H J, Yu C and Ren L L 2010 *Acta Phys. Sin.* **59** 566 (in Chinese)

[12] Chen X B and Sin J K O 2001 *IEEE Trans. Electron Devices* **48** 344

[13] Fujihira T 1997 *Jap. J. Appl. Phys.* **36** 6254

[14] Palo A 1998 *MEDICI Two-Dimensional Device Simulation Programmer User Manual* (1st Edn.) (Fremont: Avant) p. 1

[15] Mayaram K, Tien B, Hu C M and Donald O 1988 *Proc. IEDM88* December 11–14, 1988 San Francisco, USA, p. 622

[16] Ng R, Udrea F, Sheng K and Amaratunga 2001 *the 24th International Semiconductor Conference*, October 17–19, 2001 Sinaia, Romania, p. 461